Nature of phase transitions in ammonium oxofluorovanadates, a vibrational spectroscopy study of $(NH_4)_3VO_2F_4$ and $(NH_4)_3VOF_5$

Yu.V. Gerasimova[1,2], A.S. Oreshonkov[1,2], N.M. Laptash[3], A.N. Vtyurin[1,2], A.S. Krylov[1], N.P. Shestakov[1], A.A. Ershov[1,2], A.G. Kocharova[1]

[1]Laboratory of Molecular Spectroscopy, Kirensky Institute of Physics, SB RAS, Krasnoyarsk 660036, Russia

[2]Institute of Engineering Physics and Radio Electronics, Siberian Federal University, Krasnoyarsk 660079, Russia

[3]Laboratory of Optical Materials, Institute of Chemistry, FEB RAS, Vladivostok 690022, Russia

E-mail: jul@iph.krasn.ru

Abstract

Two ammonium oxofluorovanadates, $(NH_4)_3VO_2F_4$ and $(NH_4)_3VOF_5$, have been investigated by temperature-dependent infrared and Raman spectroscopy methods to determine the nature of phase transitions (PT) in these compounds. Dynamics of quasioctahedral groups was simulated within the framework of semi-empirical approach, which justified the *cis*-conformation of $VO_2F_4^{3-}$ (C_{2v}) and the C_{4v} geometry of VOF_5^{3-}. The observed infrared and Raman spectra of both compounds at room temperature (RT) revealed the presence at least of two crystallographically independent octahedral groups. The first order PT at elevated temperatures is connected with a complete dynamic disordering of these groups with only single octahedral state. At lower temperatures, the octahedra are ordered and several octahedral states appear. This PT is the most pronounced in the case of $(NH_4)_3VOF_5$, when at least seven independent VOF_5^{3-} octahedra are present in the structure below 50 K, in accordance with the Raman spectra. Ammonium groups do not take part in PTs at higher and room temperatures but their reorientational motion freezes at lower temperatures.

Keywords: ammonium oxofluorovanadates, order-disorder, dynamics, phase transitions, infrared, Raman.

PACS: 78.30.-j, 78.30.Ly

1. Introduction

The search for novel transition metal oxide fluorides is of interest since the differing bonding natures of the M–O bond and the M–F bond give rise to dramatic variations in and, potentially, fine control of the physical properties of the resulting materials. Recently, various vanadium oxide-fluoride (VOF) compounds have been proposed for use as battery (mainly, silver vanadium oxide fluorides) [1–6], nonlinear optical (NLO) materials displaying second-harmonic-generation (SHG) activity [7–9], or VOFs with magnetic responses [10–16].

Ferroelectric and proton conducting behavior of a new vanadium oxide fluoride $(NH_4,K)_3VO_2F_4$ was recently reported [17]. The compound belongs to a large structural family, namely, elpasolite and crystallizes in an orthorhombic lattice (*Immm*) at ambient temperature, similarly to $(NH_4)_3VO_2F_4$ [18]. The existence of the $VO_2F_4^{3-}$ ion in solution as well as in solid state was established by nuclear magnetic resonance (NMR) [19] and electron paramagnetic resonance (EPR) [20,21] as well as by x-ray diffraction (XRD) studies [18]. Structural studies from single crystal of $(NH_4)_3VO_2F_4$ has been reported with four kinds of disordered NH_4 groups and two types of $VO_2F_4^{3-}$ ions (one comparatively regular than the other) [18]. In accordance with the EPR data [21], one third of octahedra are dynamically disordered while the other two third represent a rigid ordered form of $VO_2F_4^{3-}$. This model structure was used for the Rietveld refinement of the observed data for $(NH_4,K)_3VO_2F_4$ [17]. Two crystallographically distinct vanadium atoms (ratio of 1:2) form two types of VO_2F_4 octahedra, with one distinguishable O and F while the other forms with indistinguishable (O,F) ligands. The model structure consists of eight crystallographically distinct anion sites with several of them have partially occupied disordered sites. Such disordering is very commonly observed in the elpasolite structure because of the orientational disorder of the octahedral units. Because the distinction of F^- and O^{2-} could not be carried out from the obtained data, the analysis of the bond distances was used to locate them. It was suggested that the V1 had a distorted octahedral arrangement with typical V–(O,F) distances as 1.69(1) x 2, 1.71(1) x 2 and 2.12(2) x 2 Å. From variation of the bond distances, the longer bond distances were assumed to be F atoms, while other four were O atoms and their spatial arrangement suggested V1 forming a *trans*-VO_2F_4 octahedra. The longer distances 1.97(1) x 2 from V2–(O,F) bond lengths were assigned to F atoms, and the octahedra were assumed to have an asymmetric *cis*-arrangement, as observed in the case of $(NH_4)_3VO_2F_4$. *Trans*-octahedral structure of VO_2F_4 in the latter case was excluded according also to experimental IR and Raman spectra of $(NH_4)_3VO_2F_4$ [18]. Crystal structure of

Ag$_3$VO$_2$F$_4$ [6] supports only *cis*-configuration of the anion. Thus, the return to *trans*-anionic structure in the case of (NH$_4$,K)$_3$VO$_2$F$_4$ [17] is not justified and the origin of four short distances assigned to the V–O bond is not clear and not consistent with the chemical formula of the compound. The incorporation of only one O atom into coordination sphere of vanadium in the related VOF (NH$_4$)$_3$VOF$_5$ should simplify and clarify the situation. In the present study, the preparation and characterization of two structural analogues of (NH$_4$)$_3$VO$_2$F$_4$ and (NH$_4$)$_3$VOF$_5$ was undertaken through vibrational spectroscopy (FTIR and Raman), especially with respect to their phase transitions (PTs).

Ammonium oxofluorovanadates (NH$_4$)$_3$VOF$_5$ and (NH$_4$)$_3$VO$_2$F$_4$ were previously assumed to be isostructural [22]. The crystal structure of the former was not determined, while the detailed single crystal structure determination of the latter performed at room temperature has revealed the orthorhombic symmetry (space group *Immm*, $Z = 6$) [18]. Clear evidences for the occurrence of the phase transitions at 418 and 215 K were obtained by variable temperature X-ray powder diffraction [18] as well as by EPR study on γ-irradiated (NH$_4$)$_3$VO$_2$F$_4$ [21]. The phase at $T > 418$ K was determined to have the cubic cryolite type structure [18]. It was also supposed that the phase transition at 215 K was of ferro- or antiferroelectric nature [21].

In accordance with the data of recent optic studies, (NH$_4$)$_3$VO$_2$F$_4$ undergoes four successive phase transitions with the following symmetry change: cubic *Fm3m* ($T_1 = 417$ K) → orthorhombic I *Immm* ($T_2 = 240$ K) → orthorhombic II ($T_3 = 211$ K) → monoclinic 112/*m* ($T_4 = 205$ K) → triclinic *P*1 [23]. The symmetry of all phases was suggested to be centrosymmetric. Calorimetric measurements performed in a wide temperature range confirmed the presence of four heat capacity anomalies at $T_1 = 438$ K, $T_2 = 244$ K, $T_3 = 210$ K, $T_4 = 205$ K associated with the first order phase transitions [24].

Heat capacity behavior $C_p(T)$ of (NH$_4$)$_3$VOF$_5$ is close to that of (NH$_4$)$_3$VO$_2$F$_4$ and associated with the succession of three phase transitions: $T_1 = 349 \pm 2$ K, $T_2 = 230 \pm 1$ K, and $T_3 = 221 \pm 1$ K. All heat anomalies are also associated with the first order transformations [25]. In accordance with our preliminary X-ray structural determinations of low-temperature phases of these compounds, no detectable changes in their crystal structures relative to those at room temperature were observed. Moreover, the O/F disorder in both structures at higher temperatures obscures the real anionic geometry. In this case, vibrational spectroscopy is very useful and helps to clear structural features of these complexes.

2. Experimental

Simple and convenient method of preparing vanadium fluorides or VOFs is a mechanochemical interaction of vanadium oxides or vanadates with ammonium hydrogen difluoride (NH_4HF_2, m.p. 126^oC) [26–29], when the reaction proceeds at ambient conditions under grinding the initial components together. We used similar reactions for synthesis of $(NH_4)_3VO_2F_4$ and $(NH_4)_3VF_6$:

$$NH_4VO_3 + 2NH_4HF_2 = (NH_4)_3VO_2F_4 + H_2O,$$
$$VF_3 + 3NH_4HF_2 = (NH_4)_3VF_6 + 3HF.$$
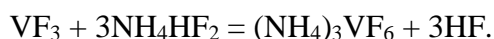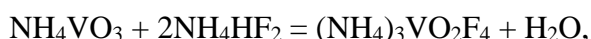
Vanadium oxides V_2O_5 and V_2O_3 can be used instead of NH_4VO_3 and VF_3 as well. All starting substances were of a reagent grade. The solid products were water-leached with addition of small amount of hydrofluoric acid (40 % HF by weight), filtered and evaporated slowly in air at room temperature. Well shaped octahedral single crystals of $(NH_4)_3VOF_5$ with bright-blue color were crystallized by slowly evaporation of the solution obtained by aqueous dissolving the stoichiometric quantities of $(NH_4)_3VO_2F_4$ and $(NH_4)_3VF_6$:

$$(NH_4)_3VO_2F_4 + (NH_4)_3VF_6 = 2(NH_4)_3VOF_5.$$
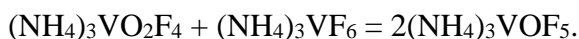
The obtained crystals of both complexes, $(NH_4)_3VO_2F_4$ and $(NH_4)_3VOF_5$, were rinsed with ethanol under vacuum and air-dried. Their compositions were checked by powder X-ray diffraction and fully corresponded to the data presented in PDF-2 (cards No. 084-1111 and 034–0882 for $(NH_4)_3VO_2F_4$ and $(NH_4)_3VOF_5$, respectively, which are virtually identical). EDX (energy-dispersive X-ray) analysis of $(NH_4)_3VOF_5$ has shown the ratio of O to F to be equal 1:5.

IR spectra were experimentally studied with vacuum Fourier-transform spectrometer VERTEX 80V (BRUKER) in spectral range 380–3500 cm^{-1} with spectral resolution 0.2 cm^{-1}. Temperature studies employed cryostat Optistat TM AC-V 12a 0.25W@4K in the temperature range from 4 to 330 K. The spectra were produced from samples in the form of tablets 13 mm in diameter and about 0.55 mm thick. The tablets were prepared as follows: the compound under study was thoroughly ground with 0.11 g of KBr in the ratio of 0.1:100. The produced mixture was vacuum pressed by hydraulic press under the pressure of 10^5 N/cm^2. Globar (silicon carbide U-shaped arc) was used as IR radiation source, with KBr beamsplitter and RT-DLaTGS as detector.

The unpolarized Raman spectra were collected in a backscattering geometry, using a triple monochromator Horiba Jobin Yvon T64000 Raman spectrometer operating in double subtractive mode, and detected by a LN-cooled charge-coupled device. The spectral reso-

lution for the recorded Stokes side Raman spectra was set to ~4 cm^{-1} (this resolution was achieved with 1800 grooves/mm gratings and 100 mm slits). The microscope system based on Olympus BX41 microscope with an Olympus 50x objective lens $f = 0.8$ mm with NA = 0.75 numerical aperture provides a focal spot diameter of about 2 μm on the sample. Single-mode argon 514.5 nm from a Spectra-Physics Stabilite 2017 Ar$^+$ laser of 5 mW on the sample was used as excitation light source. The intensity of the laser light was adjusted to avoid sample heating.

To interpret experimental spectra in the range of $VO_xF_{6-x}^{3-}$ ($x = 1,2$) internal modes we simulated dynamics of these groups using LADY software [30]. The atomic vibration frequencies were obtained using the simplified version of the Born-Karman model [31]. Only the pair-wise interactions and bond-stretching force constants A are considered; A depends on r_{ij} and the $A(r_{ij})$ dependencies are the same for all atom pairs: $A = \lambda\exp(-r_{ij}/\rho)$, where r_{ij} is the interatomic distance, and λ and ρ are the parameters characterizing the selected pair interaction.

3. Results and discussion

Fig. 1a, b shows experimental IR and Raman spectra of $(NH_4)_3VO_2F_4$ and $(NH_4)_3VOF_5$ at room temperature; these spectra can be divided into four ranges similarly to other ammonium-containing oxyfluorides [32,33].

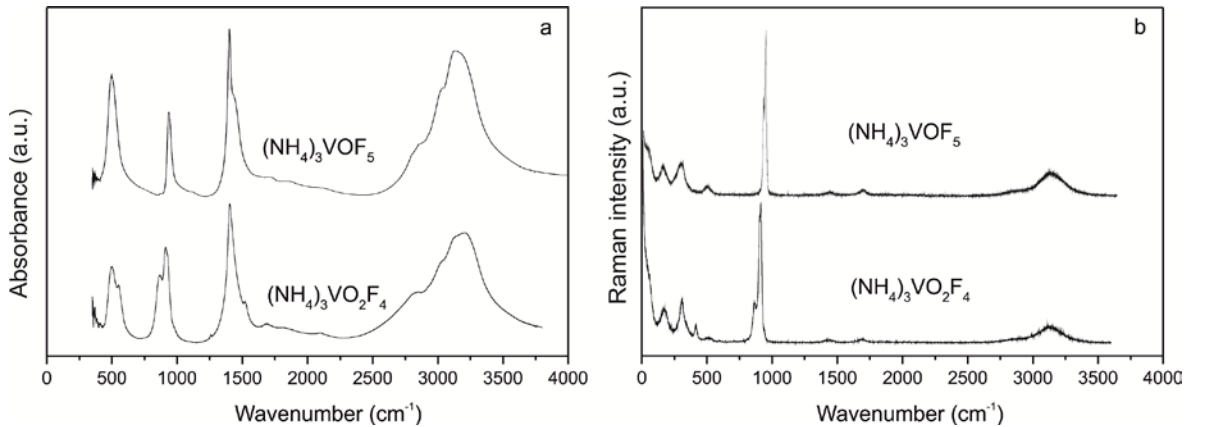**Fig. 1.** Panoramic IR (a) and Raman (b) spectra of $(NH_4)_3VO_2F_4$ and $(NH_4)_3VOF_5$ at room temperature.

Peak list of all observed bands for $(NH_4)_3VO_2F_4$ and $(NH_4)_3VOF_5$ with corresponding assignments for C_{2v} and C_{4v} octahedral geometry, respectively, and T_d for ammonium tetrahedron is presented in Table 1. Measured band frequencies at different temperatures

Table 1. Experimental wavenumbers of Raman and IR spectra of investigated compounds and their assignments

(NH$_4$)$_3$VOF$_5$		Assignment	(NH$_4$)$_3$VO$_2$F$_4$		Assignment
Raman	IR		Raman	IR	
3143	3156	ν_{as}(NH$_4$)	3133	3180	ν_{as}(NH$_4$)
2839	2839	ν_s(NH$_4$)	2822	2796	ν_s(NH$_4$)
1696		δ(NH$_4$)	1688	1688	δ(NH$_4$)
1438	1446	δ(NH$_4$)	1433	1403	δ(NH$_4$)
	1400	δ(NH$_4$)			
951	947	ν_s(VO)	914 902	928, 907	ν_s(VO$_2$)
934	932	ν_s(VO)	877 861	873, 854	ν_{as}(VO$_2$)
501	514	ν_s(VF$_4$ + VF')	507	555, 496	ν_{as}(VF$_{2c}$); ν_s(VF$_{2c}$)
	486	ν_{as}(VF$_2$)	412		δ(VO$_2$)
305		δ(VOF); r(VF$_2$ + VF')	341		ν_{as}(VF$_{2t}$) + r(VO$_2$)
264		γ(VF$_4$)	306		τ(VO$_2$+VF$_{2c}$+VF$_{2t}$); γ(VF$_{2c}$); δ(VF$_{2t}$) + γ(VF$_{2c}$); ω(VF$_{2t}$) + r(VF$_{2c}$)
162		γ(VF$_2$ – VOF')	174		ω(VF$_{2c}$) + r(VF$_{2t}$ – VO$_2$)

Symbols denote the following: ν_s – symmetric stretching vibrations, ν_{as} - asymmetric stretching vibrations, δ – bending vibrations, r – rocking, ω – wagging, τ – twisting, γ – swinging (umbrella) vibrations; F' – axial fluorine atom, VF$_{2c}$ – fluorines in *cis*-position to the O atoms, VF$_{2t}$ – fluorines in *trans*-position to the O atoms.

Spectral broad bands in the range of 2700–3500 cm^{-1} correspond to internal stretching modes of ammonium ions. Intensive IR and weak Raman lines in the range of 1400 cm^{-1} belong to the NH$_4^+$ deformation (bending) modes.

Deconvolution of the experimental spectrum in the range 850–1000 cm^{-1} shows four IR lines for (NH$_4$)$_3$VO$_2$F$_4$ and two lines for (NH$_4$)$_3$VOF$_5$ and the deconvolution of Raman spectra also shows four lines for (NH$_4$)$_3$VO$_2$F$_4$ and two for (NH$_4$)$_3$VOF$_5$ (see Table 1).

IR data for (NH$_4$)$_3$VO$_2$F$_4$ were initially published in [34]. Two IR bands were observed in the V–O stretching region at 915 and 870 cm^{-1}. These bands have been assigned

to the stretching vibrations of non-linear VO_2^+ group, meaning *cis*-conformation of VO_2F_4 octahedra. This interpretation was confirmed by Raman spectroscopy [18]. Only two strong Raman bands in the V–O stretching region at 912 and 870 cm^{-1} with their intensity ratio of 2:1 have been found.

Based on dynamics calculation of octahedral $VO_2F_4^{3-}$ with *cis*-conformation, the IR spectra in the range of 750–1000 cm^{-1} should exhibit two peaks corresponding to symmetric and antisymmetric vibrations of the V–O bonds in the area about 905 and 880 cm^{-1}, respectively. These results qualitatively agree with the data [34,18]. Deconvolution of this spectral region increases the number of active vibrations up to four lines, that can be completely described in the framework of two symmetrically independent VO_2F_4 octahedra with *cis*-configuration.

The simulation of vibrations of VOF_5 (C_{4v}) octahedron shows that the spectrum should have only one IR and one R active stretching modes. However, the IR spectra in this region consist of two lines, thus, the $(NH_4)_3VOF_5$ unit cell should contain two symmetrically independent VOF_5 octahedra as for $(NH_4)_3VO_2F_4$. Raman spectra also exhibit two intensive lines at 934 and 951 cm^{-1} (Table 1) that confirms the above item.

According to the VO_2F_4 numerical simulation, the intense Raman line at 412 cm^{-1} is assigned to the O–V–O bending mode (Fig. 2). Strong bending vibration of O–V–F (doubly degenerate) in the case of $(NH_4)_3VOF_5$ falls at 305 cm^{-1}. In the case of $(NH_4)_3VO_2F_4$, this region contains wagging, twisting, and rocking vibrations of VO_2 in combination with those of VF_{2t} and VF_{2c}. In the range of 130–200 cm^{-1} different combinations of libration modes of octahedra emerge. Their external translational and rotational vibrations modes are situated below 100 cm^{-1}.
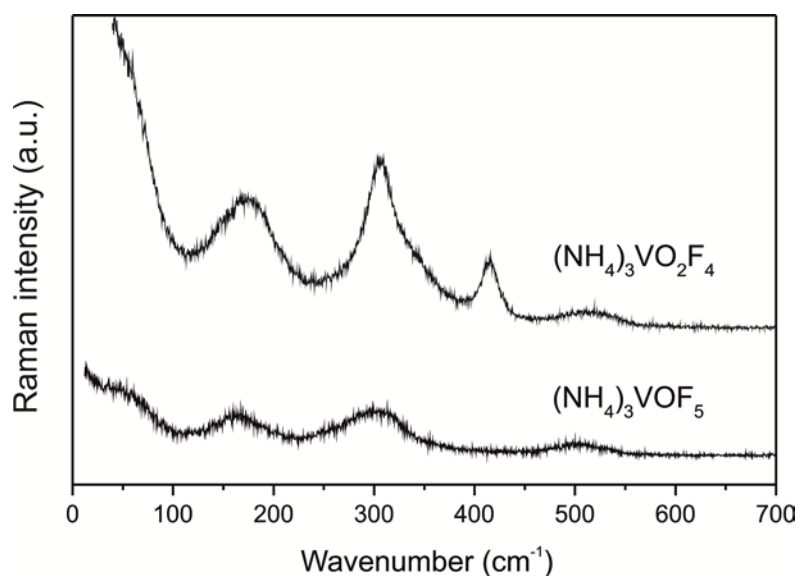

Fig. 2. Raman low frequency vibrations of $(NH_4)_3VO_2F_4$ and $(NH_4)_3VOF_5$ at RT.

Temperature transformation of low frequency vibrations of $VO_2F_4^{3-}$ and VOF_5^{3-} is shown in Fig. 3. It is seen that the width of peaks decreases while their intensity increases, which indicates the structural ordering.
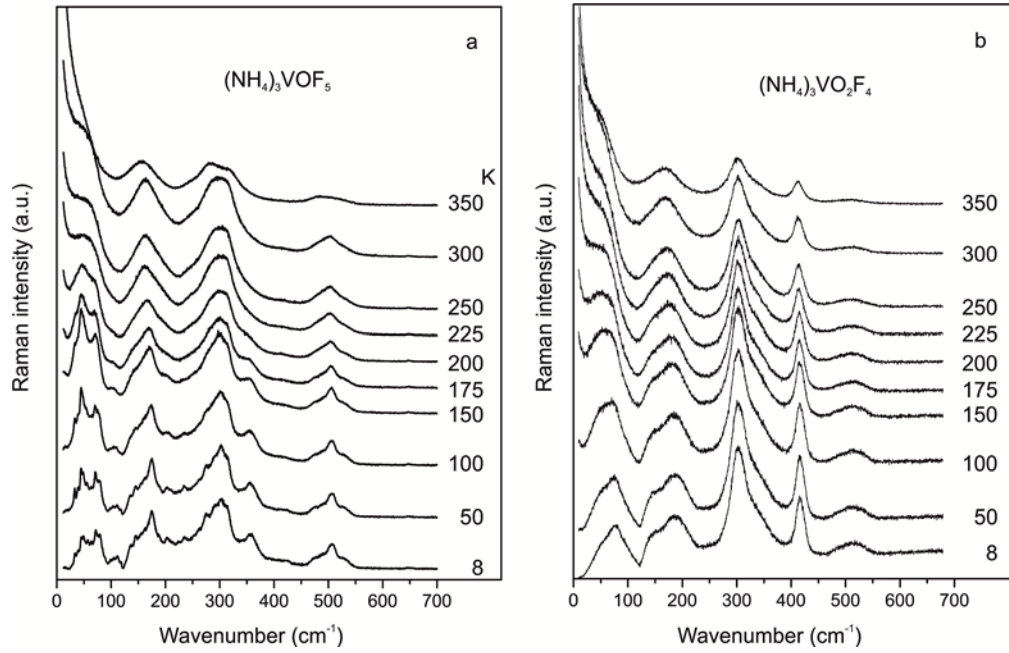

Fig. 3. Temperature transformation of low frequency vibrations of $VO_2F_4^{3-}$ and VOF_5^{3-}.

The IR spectra of $(NH_4)_3VO_2F_4$ in the range of 750–1050 cm^{-1} do not exhibit sharp anomalous behavior at the said transition temperatures. In the case of $(NH_4)_3VOF_5$, the intensity increasing of shoulder at 970 cm^{-1} is observed under cooling from the second PT (below 230 K) down to helium temperatures, Fig. 4b.
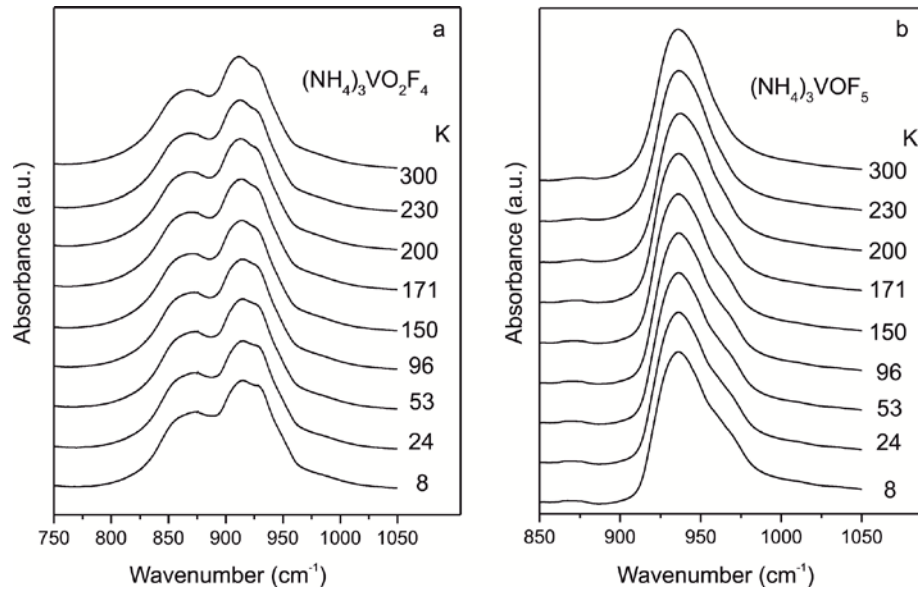

Fig. 4. Temperature transformation of high wavenumber modes in the IR spectra of $(NH_4)_3VO_2F_4$ and $(NH_4)_3VOF_5$.

Temperature transformations of the V–O stretching part of Raman spectra of $(NH_4)_3VO_2F_4$ and $(NH_4)_3VOF_5$ are shown in Fig. 5.
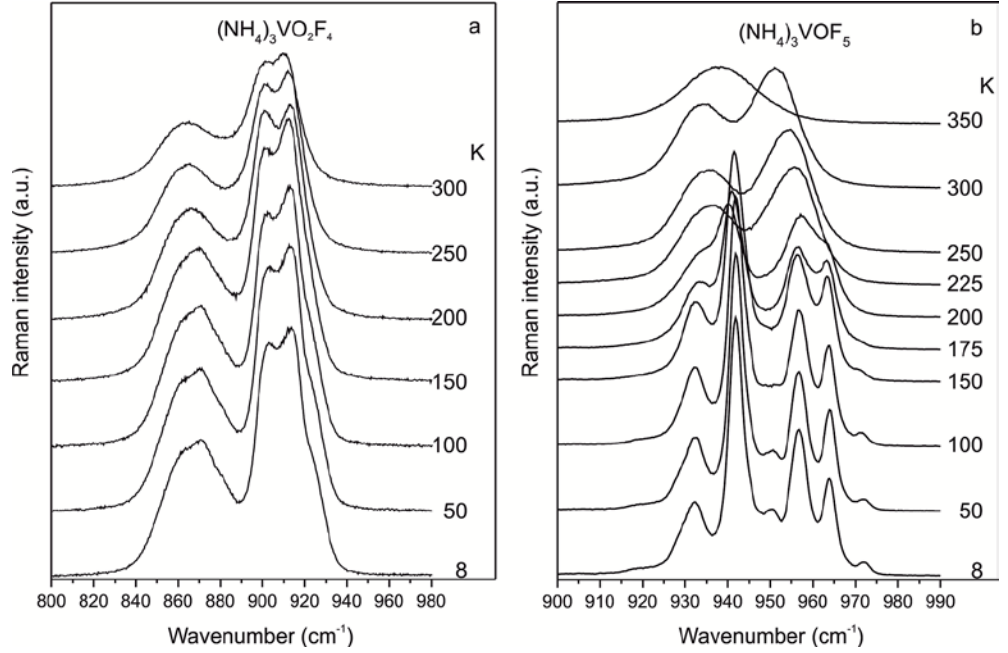

Fig. 5. Temperature transformations of high wavenumber Raman modes of $VO_2F_4^{3-}$ and VOF_5^{3-}.

Temperature changes of the $(NH_4)_3VO_2F_4$ Raman spectra are noticeable (splitting the band at 870 cm⁻¹, the emergence of shoulder at 930 cm⁻¹), but not so bright as in the case of $(NH_4)_3VOF_5$. To our best knowledge, nothing like this has been observed earlier for ammonium oxofluoro-elpasolites with a similar structure. One broad line is observed at 350 K (above the first PT point) that corresponds to a single dynamically disordered state of the VOF_5 octahedron in cubic elpasolite-like structure. The RT spectrum contains two peaks corresponding to two independent octahedral states in the orthorhombic structure. Four lines below 230 K (after the second PT) indicate the presence of at least four independent VOF_5 polyhedra with different V–O bond lengths, which means the ordering of dynamically disordered octahedra. Further cooling increases the number of lines to at least seven, which evidence about seven different local units of VOF_5 (Fig. 6) meaning full ordering of octahedral sublattice.

As was mentioned above, the mechanism of the $Fm3m \rightarrow Immm$ phase transition in the case of $(NH_4)_3VO_2F_4$ was connected with the ordering of octahedral units with the value of $\Delta S_1 = R \ln 3.2$ ($1.16R$) J mol⁻¹ K⁻¹, whereas NH_4 groups did not take part in this process [24]. Much larger ΔS values accompany PTs of other cubic ammonium oxofluoro-elpasolites such as $(NH_4)_3TiOF_5$ ($2.29R$) [35], $(NH_4)_3NbOF_6$ ($3.65R$) [36], $(NH_4)_3MoO_3F_3$

(1.61R) [37], $(NH_4)_3WO_3F_3$ (1.86R) [35]. Both orientationally disordered octahedra and ammonium tetrahedra contribute simultaneously to the entropy of PTs in these compounds.
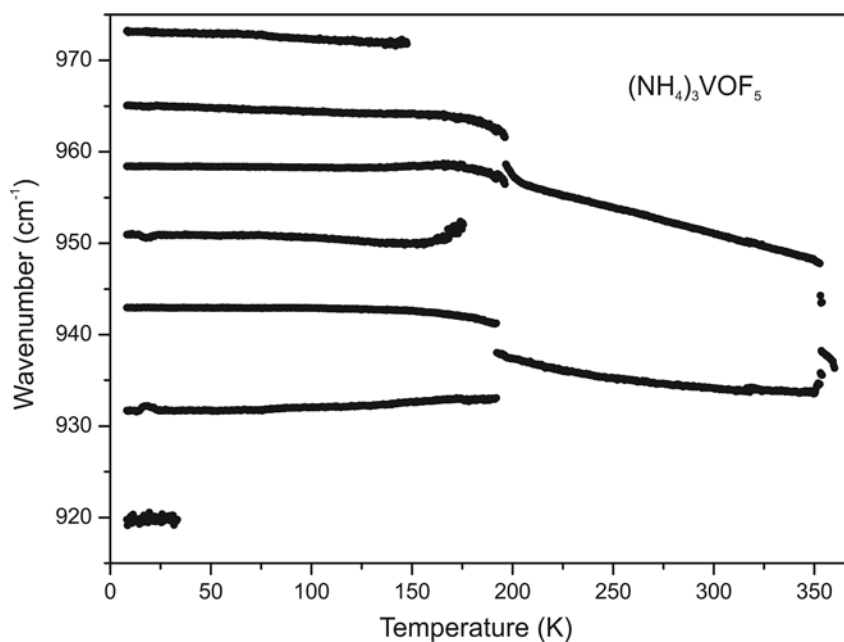

Fig. 6. Temperature dependencies of the Raman spectra of $(NH_4)_3VOF_5$ in the region of V–O stretching vibrations.

It is not surprising because polyhedra experience jumping interrelated movement in a separate microdomain [38]. Temperature-dependent Raman and infrared spectra of $(NH_4)_3MoO_3F_3$ [33,39] indicate the ordering of octahedra and ammonium groups at PTs on cooling, and the main changes take place in the region of stretching modes of Mo–O bond in accordance with the Raman spectroscopy data [39]. These features are more pronounced in the case of $(NH_4)_3WO_3F_3$ [33,40,41], which are expressed in the narrowing and splitting of the lines corresponding to vibrations of W–O bonds below the phase-transition point at 200 K.

Thermal behavior of $(NH_4)_3VO_2F_4$ and $(NH_4)_3VOF_5$ should be also compared with that of $(NH_4)_2WO_2F_4$ and $(NH_4)_2MoO_2F_4$. The latter two compounds crystallize in orthorhombic symmetry (*Cmcm*) and are characterized by two independent states of a *cis*-MO_2F_4 (M = Mo, W) octahedron statically and dynamically disordered in their structures [42,43]. The crystal structures at room temperature are very similar and differ only by the ratio of the static and dynamic components of orientational disorder. Octahedral groups and ammonium tetrahedra (two independent groups) reorient independently (in contrast to cubic ammonium fluoroelpasolites). At low temperature the two complexes undergo order-disorder phase transitions from dynamic states to static states. These PTs are accompanied by rather large ΔS values: $R \ln 9.8$ (2.28R) and $R \ln 8.9$ (2.19R) for $(NH_4)_2WO_2F_4$ (201 K)

and $(NH_4)_2MoO_2F_4$ (270 K), respectively [44,45]. After the phase transition the anionic sublattice in the two complexes transform to the rigid state, but the octahedra are fully ordered in $(NH_4)_2WO_2F_4$ while they are statically disordered in $(NH_4)_2MoO_2F_4$. Ammonium groups are fully ordered in the low-temperature phase of $(NH_4)_2MoO_2F_4$ (all hydrogen atoms were localized), while they partially move (reorient) in the low-temperature phase of $(NH_4)_2WO_2F_4$ [43]. The ordering of octahedral groups and partial ordering of ammonium groups during the PT in $(NH_4)_2WO_2F_4$ and $(NH_4)_2MoO_2F_4$ was recently confirmed by Raman spectroscopy [46,47]. The significant spectra changes were observed in the range corresponding to the M−O (M = Mo, W) vibrations, while the noticeable changes corresponding to the ammonium vibrations have been found below the second PT at 160 K (W) and 180 K (Mo).

The changes in the Raman and infrared spectra of the NH_4 stretching and bending vibrations of $(NH_4)_3VOF_5$ with temperature are presented in Fig. 7. With the temperature decreasing below 230 K the spectral profile becomes complex. However, the main changes in the range of the NH_4 vibrations occur below the third phase transition. Large linewidths in cubic and orthorhombic phases, corresponding to the internal stretching and bending vibrations of the NH_4 ion, can be due to both the influence of the well known anharmonicity of NH_4^+ ion vibrations and the orientational disordering of ammonium sublattices. Spectral bands split after decreasing temperature below 221 K. The phenomena observed can be accounted for the ordering of the ammonium groups below the third phase transition.

In the case of $(NH_4)_3VO_2F_4$, changes of spectral parameters become visible below 200 K (Fig. 8). Ammonium tetrahedra are ordered at low temperatures, which is consistent with the calorimetric data [24]. Tetrahedra participate in the low-temperature PT, which results in complete ordering of ammonium sublattice.
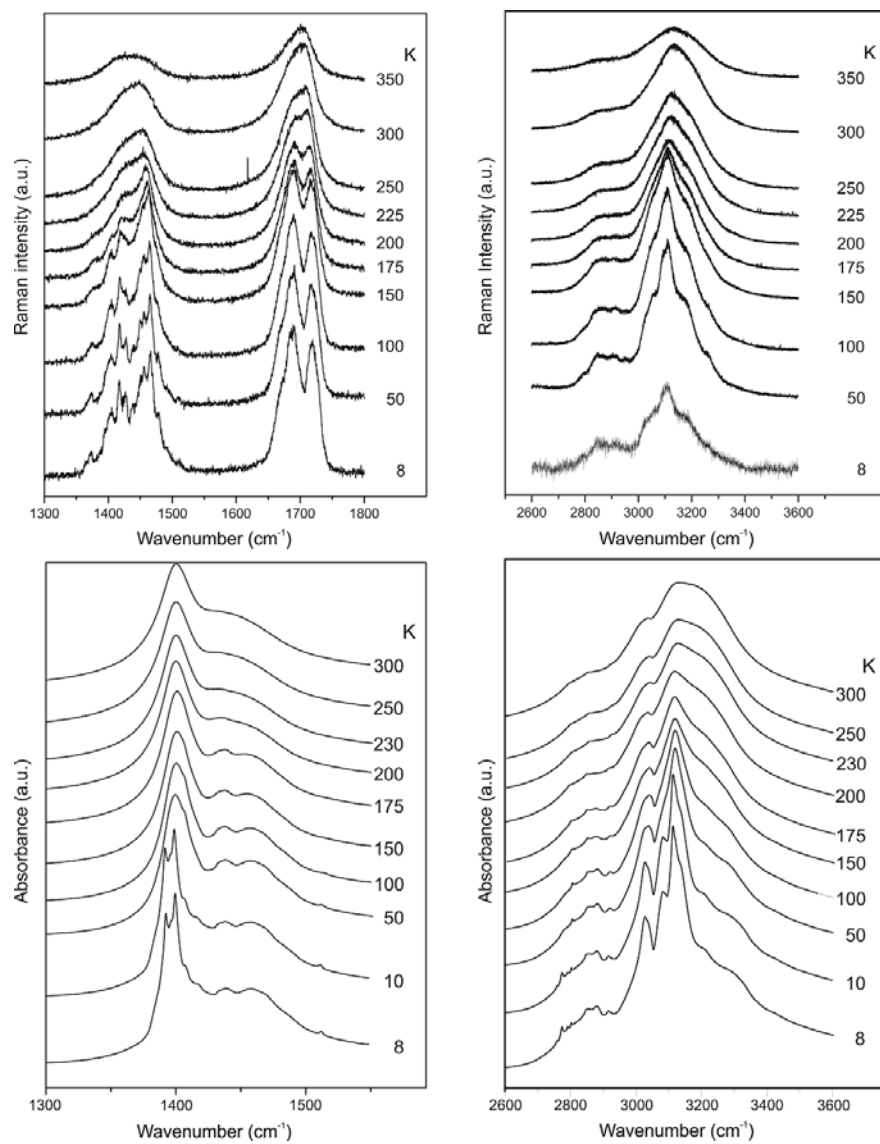
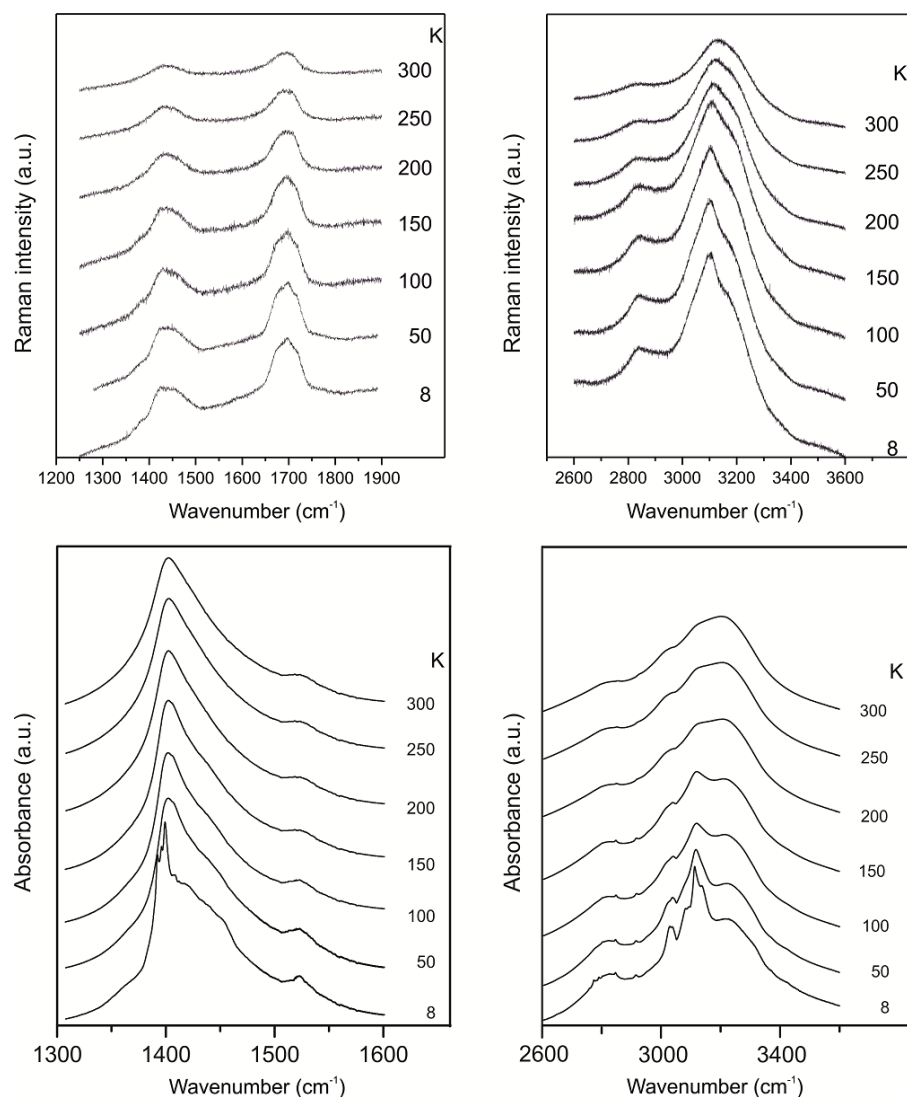Fig. 7. Raman and IR active lines related to bending and stretching vibrations of ammonium ions in $(NH_4)_3VOF_5$.

Fig. 8. Raman and IR active lines related to bending and stretching vibrations of ammonium ions in $(NH_4)_3VO_2F_4$.

4. Conclusion

The dynamic nature of phase transitions in two isostructural ammonium oxofluorovanadates, $(NH_4)_3VO_2F_4$ and $(NH_4)_3VOF_5$, has been investigated by temperature-dependent infrared and Raman spectroscopy. In difference with available literature data concerning vibrational spectra of $(NH_4)_3VO_2F_4$ [18,34,48], our spectral data clearly demonstrate the existence of two octahedral states at RT in crystal structures of both, $(NH_4)_3VO_2F_4$ and $(NH_4)_3VOF_5$, compounds. The most pronounced structural changes during the PTs are reflected in the Raman spectra of $(NH_4)_3VOF_5$. This is a unique case of spectral transformations not observed till now for oxofluoro-elpasolites with a similar structure. The first PT at higher temperature is connected with the transition into a single dynamically disordered state of oxofluoro-polyhedra in cubic elpasolite-like structure.

13

Ammonium groups do not participate in this process in difference with other cubic fluoro- or oxofluoro-elpasolites with jumping interrelated movement of both orientationally disordered octahedra and ammonium tetahedra contributing simultaneously to the entropy of PTs.

On cooling, the second PT in ammonium oxofluorovanadates is accompanied by the further ordering of orientationally disordered anionic sublattice. This behavior resembles that for $(NH_4)_2MoO_2F_4$ and $(NH_4)_2WO_2F_4$ with the coexistence of static and dynamic orientational disorder at RT. Octahedral groups and ammonium tetrahedra reorient independently, so that on cooling the order-disorder PT from dynamic to static state with completely ordered octahedra. Ammonium tetrahedra are fully ordered in the low-temperature phase of $(NH_4)_2MoO_2F_4$ or they partially move (reorient) in the low-temperature phase of $(NH_4)_2WO_2F_4$. One can suppose that in ammonium oxofluorovanadates, octahedra continue to be ordered at lower temperature (at least four independent VOF_5 octahedra at 230–200 K) and they are fully ordered below 35 K (at least seven different octahedral in the crystal structure of $(NH_4)_3VOF_5$). At this temperature a complete freeze of reorientational motion of ammonium groups takes place in $(NH_4)_3VOF_5$, as well as in $(NH_4)_3VO_2F_4$.

Cis-structure of $VO_2F_4^{3-}$ is doubtless, so its *trans*-configuration in the case of $(NH_4,K)_3VO_2F_4$ [17] should be excluded. We hope that the obtained results will help to refine intricate structures of the complexes under consideration.

Acknowledgments

References

[1] E. M. Sorensen, H. K. Izumi, J. T. Vaughey, C. L. Stern, K. R. Poeppelmeier, J. Am. Chem. Soc. 127 (2005) 6347–6352.

[2] T. A. Albrecht, C. L. Stern, K. R. Poeppelmeier, Inorg. Chem. 46 (2007) 1704–1708.

[3] M. Bertoni, N. Kidner, T. Mason, T. Albrecht, E. Sorensen, K. Poeppelmeier, J. Electroceram. 18 (2007,) 189–195.

[4] F. Sauvage, V. Bodenez, H. Vezin, T.A. Albrecht, J.-M. Tarascon, K.R. Poeppelmeier, Inorg. Chem. 47 (2008) 8464–8472.

[5] T. A. Albrecht, F. Sauvage, V. Bodenez, J.-M. Tarascon, K.R. Poeppelmeier, Chem. Mater. 21 (2009) 3017–3020.

[6] J. M. Chamberlain, T. A. Albrecht, J. Lesage, F. Sauvage, C. L. Stern, K. R. Poeppelmeier, Cryst. Growth Des. 10 (2010) 4868–4873.

[7] N. F. Stephens, M. Buck, P. Lightfoot, J. Mater. Chem. 15 (2005) 4298–4300.

[8] M. D. Donakowski, R. Gautier, J. Yeon, D. T. Moore, J. C. Nino, P. S. Halasyamani, K. R. Poeppelmeier, J. Am. Chem. Soc. 134 (2012) 7679–7689.

[9] M. D. Donakowski, R. Gautier, H. C. Lu, T. T. Tran, J. R. Cantwell , P. S. Halasyamani, K.R. Poeppelmeier, Inorg. Chem. 54 (2015) 765–772.

[10] D. W. Aldous, R. J. Goff, J. P. Attfield, P. Lightfoot, Inorg. Chem. 46 (2007) 1277–1282.

[11] T. Mahenthirarajah, P. Lightfoot, Chem. Commun. (2008) 1401–1403.

[12] D. W. Aldous, P. Lightfoot, Solid State Sci. 11 (2009) 315–319.

[13] K. Adil, M. Leblanc, V. Maisonneuve, P. Lightfoot, Dalton Trans. 39 (2010) 5983–5993.

[14] F. Himeur,P. K. Allan,S. J. Teat, R. J. Goff, R. E. Morris, P. Lightfoot, Dalton Trans. 39 (2010)6018–6020.

[15] M. D. Donakowski, H. C. Lu, R. Gautier, R. Saha, A. Sundaresan, K. R. Poeppelmeier, Z. Anorg. Allg. Chem. 640 (2014) 1109–1114.

[16] J. G. Yeon, J. B. Felder, M. D. Smith, G. Morrison, H. -C. zur Loye, CrystEngComm. 17 (2015) 8428–8440.

[17] S. J. Patwe, S. N. Achary, K. G. Girija, C. G. S. Pillai, A. K. Tyagi, J. Mater. Res. 25 (2010) 1251–1263.

[18] M. Leimkühler, R. Mattes, J. Solid State Chem. 65 (1986) 260–264.

[19] R. J. Gillespie, U. R. K. Rao, J. Chem. Soc., Chem. Commun. (1983) 422–423.

[20] S. V. Adhyapak, R. M. Kadam, A. G. Page, U. R. K. Rao, Phase Transit. 51 (1994) 199–208.

[21] U. R. K. Rao, K. S. Venkateswarlu, B. R. Wani, M.D. Sastry, A. G. I. Dalvi, B. D. Joshi, Mol. Phys. 47 (1982) 637–645.

[22] R. L. Davidovich, L. G. Kharlamova, L. V. Samarets, Koord. Khim. 3 (1977) 850–856.

[23] S. V. Melnikova, A. G. Kocharova. Phys. Solid State, 51 (2009) 597–600.

[24] V. D. Fokina, M.V. Gorev, A. G. Kocharova, E. I. Pogoreltsev, I. N. Flerov, Solid State Sci. 11 (2009) 836–840.

[25] E. I. Pogoreltsev, private communication.

[26] B. N. Wani, U. R. K. Rao, K. S. Venkateswarlu, A. S. Gokhale, Thermochim. Acta 58 (1982) 87–95.

[27] B. N. Wani, U. R. K. Rao,Synth. React. Inorg. Met-Org. Chem. 21, *5* (1991) 779–791.

[28] B. N. Wani, U. R. K. Rao, J. Solid State Chem. 94 (1991) 428–431.

[29] B. N. Wani, U. R. K. Rao, Mater. Chem. Phys. 33 (1993) 165–167.

[30] M. B. Smirnov, V. Yu. Kazimirov, Lady. Software for lattice dynamics simulations. Communication of the Joint Institute for Nuclear Research, Dubna, 2001.

[31] M. Smirnov, R. Baddour-Hadjean, Li intercalation in TiO_2 anatase: Raman spectroscopy and lattice dynamic studies, J. Chem. Phys. 121 (2004) 2348–2355.

[32] A. N. Vtyurin, Yu. V. Gerasimova, N. P. Shestakov, A. A. Ivanenko, Phys. Solid State 53 (2011) 840–844.

[33] A. N. Vtyurin, Yu. V. Gerasimova, A. S. Krylov, A. A. Ivanenko, N.P. Shestakov, N. M. Laptash, E. I. Voyt, J. Raman Spectr. 41 (2010) 1784–1791.

[34] R. L. Davidovich, V. I. Sergienko, L. M. Murzakhanova, Russ. Chem. Bull., Siberian Branch Acad. Sci. USSR 2 (1968) 58–61.

[35] I. N. Flerov, V. D. Fokina, A. F. Bovina, N. M. Laptash, Solid State Sci. 6 (2004) 367–370.

[36] V. D. Fokina, I. N. Flerov, M. V. Gorev, E. V. Bogdanov, A. F. Bovina, N. M. Laptash, Phys. Solid State 49 (2007) 1548–1553.

[37] I. N. Flerov, V. D. Fokina, A. F. Bovina, E. V. Bogdanov, M. S. Molokeev, A. G. Kocharova, E. I. Pogoreltsev, N. M. Laptash, Phys. Solid State 50 (2008) 515–524.

[38] A. A. Udovenko, N. M. Laptash, Acta Cryst. B64 (2008) 305–311.

[39] A. S. Krylov, S. N. Krylova, A. N. Vtyurin, N. M. Laptash, A. G. Kocharova, Ferroelectrics 430 (2012) 65–70.

[40] Yu. V. Gerasimova, A. N. Vtyurin, A. S. Krylov, A. A. Ivanenko, N. P. Shestakov, N. M. Laptash, Bull. Rus. Acad. Sci.: Physics 72 (2008) 1145–1148.

[41] K. S. Aleksandrov, A. N. Vtyurin, Ju. V. Gerasimova, A. S. Krylov, N. M. Laptash, E. I. Voyt, A. G. Kocharova, S. V. Surovtsev, Ferroelectrics 347 (2007) 79–85.

[42] A. A. Udovenko, N. M. Laptash, Acta Cryst. B64 (2008) 645–651.

[43] A. A. Udovenko, A. D. Vasiliev, N. M. Laptash, Acta Cryst. B66 (2010) 34–39.

[44] I. N. Flerov, V. D. Fokina, , M. V. Gorev, A. D. Vasiliev, A. F. Bovina, M. S. Molokeev, A. G. Kocharova, N. M. Laptash, Phys. Solid State, 48 (2006) 759–764.

[45] V. D. Fokina, E. V. Bogdanov, E. I. Pogoreltsev, V. S. Bondarev, I. N. Flerov, N. M. Laptash, Phys. Solid State 52 (2010) 158–166.

[46] A. S. Krylov, S. V. Goryainov, N. M. Laptash, A. N. Vtyurin, S. V. Melnikova, S. N. Krylova, Cryst. Growth & Des. 14 (2014) 374–380.

[47] A. Krylov, N. Laptash, A. Vtyurin, S. Krylova, J. Mol. Struct. 1124 (2016) 125–130.

[48] D. de Waal, A. M. Heyns, Proc. SPIE 2089, 9th International Conference on Fourier Transform Spectroscopy, Calgary, Canada (1993) 204–205.